

Methane Emission from Palsa Mires in Northeastern European Russia

M. N. Miglovets^{a*}, S. V. Zagirova^a, N. N. Goncharova^a,
and O. A. Mikhailov^a

^a*Institute of Biology, Komi Scientific Center, Ural Branch, Russian Academy of Sciences,
ul. Kommunisticheskaya 28, Syktyvkar, 167982 Russia*

**e-mail: miglovets@ib.komisc.ru*

Received July 15, 2019

Revised December 27, 2019

Accepted October 19, 2020

Abstract—Measurement data on methane fluxes in the palsa mire ecosystem at the border of tundra and taiga zones in northeastern European Russia are presented. It was found for the first time that an intense methane flux from the surface of the permafrost mound (palsa) is determined by the spring thawing of the seasonally thawed horizon in the layer of 14–25 cm. During this period, the emission was 4–20 times higher than the summer values. In lichen communities of peat mounds, the CH₄ sink prevailed during the summer-autumn period. The total methane flux in different parts of the mire in June–September varied from 0.18 to 16.5 kg CH₄/ha. In general, the palsa mire emitted 81 kg CH₄/ha per year to the atmosphere. The methane emission from the surface of peat mounds and hollows made up 20% and 80% of the annual flux, respectively.

DOI: 10.3103/S1068373921010076

Keywords: Extreme northern taiga subzone, palsa mire, methane flux, discontinuous permafrost

INTRODUCTION

The carbon stock in the Arctic and subarctic wetlands is 2050 Pg (1 Pg = 10⁹ t) [18]. An increase in the emission of carbon in the form of CO₂ and CH₄ up to 37–174 Pg is expected by 2100 due to the climate warming and permafrost thaw. Despite an insignificant (2–3%) contribution of methane to the total carbon emission from the high-latitude wetlands, its impact on climate can make up 35–48% due to the greenhouse potential as compared to CO₂ [29].

The area of wetlands in Russia is 1.39 · 10⁶ km², 14.6% of this area is occupied by permafrost mound (palsa) mires [2]. In the European part of Russia, such mires are common in the regions with average annual air temperature about –1 °C and total annual precipitation <500 mm. The width of the zone of palsa mires in European Russia is 50–100 km on the Kola Peninsula, 200–300 km in the north of the Komi Republic and Nenets Autonomous Okrug. The southern boundary of palsa mires coincides with the border between forest tundra and northern taiga zones [30]. According to the regional plant classification, palsa mires belong to the group of European-West Siberian grass-lichen-moss swamps [9]. The formation of mounds and their shape is determined by underlying permafrost. Large mounds (with a height to 4 m) and complexes formed of them occupy a small area of the wetland, where fen and mound-hollow complexes, as well as peat deposits (more often, lowland ones) dominate [8].

Palsa mires are a convenient model for studying a response of land ecosystems to climate change. It is shown that carbon loss due to methane emission in the ecosystems of this type of wetlands in Northern Europe varies from –0.9 mg C-CH₄/(m² day) at mounds to 42 mg C-CH₄/(m² day) in grassy fens [22]. In the tundra zone in Western Siberia, total methane emission from palsas was equal to 1.9 · 10³ t C-CH₄ per year, which corresponded to 1% of total emission from all wetlands [10]. For northeastern European Russia, carbon fluxes from tundra wetlands have been explored [16], but the role of palsa mires in the methane emission is still unexplored.

The objective of the present paper is to reveal the seasonal dynamics of the methane flux from the surface of various microlandscapes of the palsa mire during the snowless season.

OBJECTS AND METHODS OF RESEARCH

The measurements of the methane flux were carried out in 2016 at the palsa mire located at the watershed of the Chernaya and Bol'shaya Inta rivers (65 54 10 N, 60 26 40 E, the Komi Republic). The study area is situated in the zone of moderately cold summer, where the sum of temperatures above 10 °C varies from 600 to 900 °C [1]. Total precipitation is 500–600 mm for the warm season and 200–250 mm for the cold one. The average date of formation of the seasonal snow cover is October 15–20, the average snow depth is 60 cm.

The study area is situated at the southern boundary of permafrost, structured ice is preserved only in peat mounds and is absent in hollows [4]. Dry-peat permafrost soils are formed at the mounds, and peat oligotrophic non-permafrost soils are formed in depressions between the mounds [7].

The description of the vegetation cover is performed using the geobotanic methods [12], and the area of the main types of microlandscape (microsites) was determined using Landsat 8 satellite images. The area of the explored part of the palsa mire is 11 ha, including 3.4 ha of palsas (of them, 0.6 ha of peat spots), 3.7 ha of hollows and fens, 3.9 ha of ridges, 0.2 ha of water bodies. The palsa mire is characterized by two types of microsites: (1) the ridge-hollow one: *Ledum palustre*, *Vaccinium uliginosum*, *Empetrum hermaphroditum*, *Rubus chamaemorus*, *Sphagnum fuscum* species dominate at the ridges, and *Eriophorum russeolum*, *Carex limosa*, *C. rotundata* grasses and *Sphagnum lindbergii*, *S. riparium* mosses prevail in the hollows; (2) permafrost peat mounds with a height of 3–4 m, at whose top lichen, shrub-lichen phytocenoses, and greenless peat spots (to 30% of the mound area) are formed; the plant communities are dominated by *Ledum palustre*, *Vaccinium uliginosum*, *Betula nana*, *Empetrum hermaphroditum*, the moss-lichen layer is dominated by *Cladonia arbuscula*, *C. coccifera*, *C. gracilis*, and *C. rangiferina* lichens with the projective cover of 60%.

Daily and seasonal measurements of the methane flux were carried out during 3–4 days of every month in May–September 2016 using the static dark chamber method in the communities typical of the mire: shrub-sphagnum oligotrophic ridges ($n = 22$), cotton-grass-sphagnum hollows ($n = 23$), shrub-lichen communities ($n = 30$), and exposed peat spots ($n = 19$) of the palsa. The chamber volume is 0.1 m³, the area of the stationary base with hydraulic lock is 0.25 m². The chamber exposure time was 20 minutes. The volume fraction of methane (ppm) was determined with the UGGA-30p portable gas analyzer (Los Gatos Research, USA). The methane flux was calculated using the equation

$$F_{\text{CH}_4} = \frac{P \cdot V \cdot M}{R \cdot (273 + T) \cdot A} \cdot k / 1000 \quad (1)$$

where F_{CH_4} is the methane flux, mg/(m² hour); P is air pressure at the moment of measurement, Pa; V is the chamber volume, m³; M is the molar mass of methane (16.043 g/mol); R is the gas constant (8.314472 Pa m³/mol K), T is temperature inside the chamber of the measurement moment, °C; A is the area of the frame limiting the surface, m²; k is the slope coefficient of the linear function of temporal variations in the gas concentration in the form of $kx + b$, ppm/hour; 1000 is the coefficient of conversion of micrograms to milligrams.

The total seasonal methane flux was estimated using the seasonal median of daily fluxes according to [11]:

$$F_{\text{tot}} = \text{Me} \cdot R_c \cdot n \quad (2)$$

where F_{tot} is the total flux per n days from a unit area of the analyzed community-facie, g CH₄/m²; Me is the median of the methane flux from the surface of the investigated community per season, mg CH₄/(m² hour); R_c is the coefficient of conversion of mg/hour into g/day, equal to 0.024; n is the length of the calculation period that corresponded to the number of days from the stable upward 5 °C crossing in average daily air temperature till the downward 0 °C crossing.

The calculation period in 2016 was 163 days, which corresponds to the period of active methane emission exceeding the duration of the summer-autumn season by 12% [11]. The deviation of the value of daily fluxes did not exceed 25% of the daily median ($n = 5$).

Temperature in the active layer of the peat mound was registered with S-TMB-M006 sensors (Onset, USA) (the error is 0.2 °C) installed under the lichen cover on the ground surface and at the depth of 15 and 20 cm. Temperature was recorded at the depth of 25 cm in hollows, in the upper 7-cm layer of moss (aerobic conditions), and at the depth of 25–30 cm (anaerobic conditions) at ridges. At the mound, the

Table 1. Microclimatic and edaphic characteristics at the palsa mire during the observation period in 2016

Month	T_a	T_a	Q , %	T_{GS}	T_{20}	Z , mm/day	WTL	f , %
	C			C				
May	5.3	4.8	76	6.8	0.1	2.6	–	23.1
June	12.8	3.7	188	10.5	0.2	5.2	–2.6 (–7)	21.9
July	19.8	5.7	52	18.4	3.6	7.8	–16.7 (–24)	15.7
August	15.8	4.8	132	14.4	6.2	5.9	–13.5 (–20)	17.9
September	9.2	3.9	72	8.4	4.2	4.4	–11.3 (–16)	18.0

Note: T_a is monthly mean air temperature; T_a is its deviation from the normal (according to [5]); Q is total precipitation (percentage of the normal) [5]; T_{GS} and T_{20} are monthly mean temperature on the surface of ground and active peat layer to the depth of 20 cm (the values for the palsa are given); Z is the rate of thawing of the seasonally thawed layer, $Z = (Z_n - Z_1)/n$, where n is the number of days in the computational month; WTL is the mean water table level (monthly mean data were obtained for a part of the cotton-grass-sphagnum hollow, the minimum for each month is given in brackets); f is the average moisture content in the upper peat layer.

S-SMC-M005 sensors (the error is 3.1%) were used to determine the moisture content in the upper 10-cm peat layer; air temperature and relative air humidity were measured at the height of 1.5 m with the S-THB-M002 sensors (the error is 0.21 °C and 2.5%, respectively). The thaw depth of the palsa was determined with a metal probe. The variations in thaw depth during a season were retrieved from the regression equations:

$$Z_{PS} = 10.7 + 0.006TDD, \quad (3)$$

$$Z_{LC} = 14.1 + 0.005TDD \quad (4)$$

where Z_{PS} and Z_{LC} are thaw depth on the peat spot and under the lichen community of the palsa, respectively, cm; TDD is the sum of accumulated positive air temperatures. The presented equations (3), (4) reliably verified the thaw depth dynamics based on empirical data (the coefficient of determination $R^2 = 0.96$ at $p < 0.000$, $n = 12$).

The parameter TDD was calculated according to [21] using the formula

$$TDD = \sum_{i=1}^n T_i \quad (5)$$

where T_i is averaged daily air temperature, °C; $C_i = 1$ if $T_i > 0$ and $n = 0$ if $T_i < 0$, n is the number of days in the calculation period (83 days).

RESULTS AND DISCUSSION

Weather conditions and thaw depth dynamics. In May–August in 2016, the monthly mean values of air temperature were 3.7–5.7 °C above the multiyear means for 1940–2006 (Table 1). Heavy rains were observed in June and August, July was characterized by significant precipitation deficiency. The maximum temperature was recorded in July, when the mire water level in hollows dropped to –24 cm, and temperature at the depth of 20 cm was 16 °C. The differences in the seasonal temperature variations were found for different horizons of the palsa peat deposit (Fig. 1). Temperature on the peat deposit surface and at the depth of 15 cm corresponded to the air temperature variation. The thawing of the upper horizon of the mound started during the first ten days of April at average daily air temperature of 4 °C, the dramatic temperature rise was registered during the third ten days of May, and its maximum was observed at the beginning of July. At the depth of 20 cm in May–June, temperature of the peat mound was close to 0 °C, its maximum was shifted to the middle of August. At the beginning of October, the temperature inversion occurred in the peat deposit, and positive temperature at the depth of 20 cm was kept till the first ten days of December at the freezing of the upper horizons. The thaw depth in the middle of September was 78 cm. The minimum moisture content at the upper horizon of the peat mound was observed in July (Table 1).

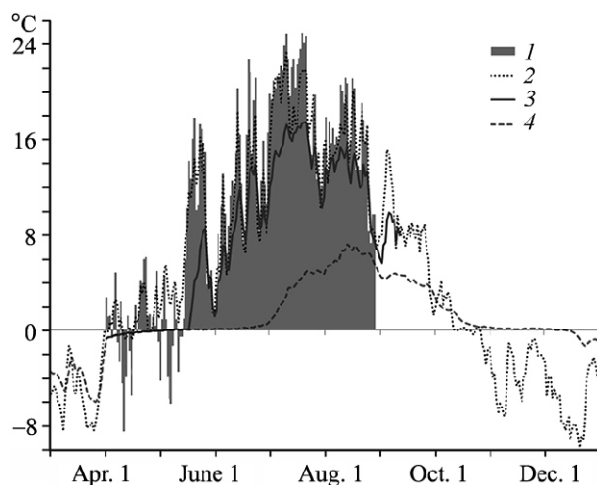


Fig. 1. The seasonal dynamics of average daily air temperature (1) at the height of 1.5 m and at the palsa peat deposit ((2) on the surface (0–3 cm), (3) at the depth of 15 cm, (4) at the depth of 20 cm) in March–December in 2016.

Seasonal variations in methane fluxes. The methane flux from the peat mound varied during the season within $-0.19...3.8$ mg/(m² hour), and that from grassy hollows and shrub ridges was within $0.4–26$ mg/(m² hour) (Table 2). The methane emission from the cotton-grass-sphagnum hollows was associated with air temperature (the correlation coefficient $r = 0.54$, $p < 0.01$), the maximum was registered in July, which agrees with the studies of other types of tundra and boreal wetland ecosystems [17, 20, 28]. High temperature of air and peat has a positive effect on the root exudation, which is the main way to increase the easily accessible substrate in the rhizosphere for acetoclastic representatives of methanogenic archaea [13]. The negative correlation was revealed between the seasonal variations in methane fluxes and mire water level in hollows ($r = -0.68$, $p < 0.01$). Extremely high values of methane emission were observed at the water level below -20 cm, which may be associated with the inclusion of CH₄ bubble transport and with an increase in methane concentration with a decrease in hydrostatic pressure against a background of the water level drop [26]. The observations of the linear growth of grass in cotton-grass-sphagnum hollows in a palsa mire by the “tying” method demonstrated a reliable correlation between the methane flux and the mass of overground organs of *Eriophorum russeolum* and *Carex limosa* ($r = 0.84$, $p < 0.002$), which may be associated with their ability to conduct from 37 to 90% of the daily methane flux through the aerenchyma of axial organs [27, 32].

The seasonal dynamics of methane emission is less clearly pronounced for the communities of shrub ridges and permafrost peat mound. The flux from the mound surface in May varied within $0.02–3.8$ mg/(m² hour), with the median of 1.07 mg/(m² hour), which corresponds to the spring emission of CH₄ from shrub-sphagnum ridges, but it is significantly smaller than emission from grass communities (Table 2). In the next months, the methane flux from the palsa did not exceed 0.26 mg/(m² hour). The shrub-lichen communities of the mound in 60% of cases were the sink of atmospheric methane (Table 2), which could be caused by the high volume density of peat impeding the methane diffusion from the deeper layers of the mound and by the activity of the complex of methanotrophic bacteria in the surface active layer of peat [25].

During the initial period of formation of the seasonally thawed layer, a spring surge of methane flux from the surface of the palsa was observed, which some authors associate with the release of gas accumulated in autumn [25]. The possibility of residual methanogenesis in autumn is indicated by the laboratory experiments, when 3–15 ppm of methane was preserved in the pores of the active peat layer at the temperature drop from 0 to -1 °C [31]. The maximum concentration (63 ppm) was recorded at the moment of peat thaw simulation at the temperature rise to 2–6 °C. According to the observations at the palsa mire, after the autumn inversion, positive temperature in the 20-cm peat layer was maintained till December (Fig. 1), which created conditions for methanogenesis. The generated gas was accumulated and conserved in ice crystals, its release to the atmosphere occurred at the beginning of formation of the seasonally thawed layer next spring.

Table 2. The methane flux from the surface of the palsa mire elements

Month	<i>n</i>	<i>s</i> , %	CH ₄ , mg/(m ² hour)				
			Me	min	max	\bar{x}	
Peat spots (palsa)							
May	4	6	0.889	0.02	3.16	0.985	0.963
June	4		0.036	0.03	0.26	0.068	0.089
July	3		0.099	0.02	0.25	0.124	0.091
August	3		0.244	0.14	0.26	0.215	0.065
September	3		0.007	-0.04	0.10	0.014	0.039
June–September			0.04				
Lichen communities (palsa)							
May	4	25	1.07	0.22	3.85	1.35	1.08
June	4		-0.07	-0.17	0.07	-0.06	0.08
July	3		0.09	-0.11	0.21	0.048	0.12
August	3		-0.04	-0.19	0.12	-0.05	0.11
September	3		-0.06	-0.12	-0.007	-0.08	0.08
June–September			-0.06				
Cotton-grass-sphagnum hollow							
May	4	33.3	3.72	3.3	4.3	3.78	0.96
June	4		5.9	4.5	6.8	6.01	1.9
July	3		10.2	6	16.8	12.7	9.7
August	3		2.83	2.1	3.5	2.8	0.87
September	3		3.69	3	4	3.3	1.08
June–September			4.16				
Shrub-sphagnum ridge							
May	4	35.7	1.25	0.8	1.76	1.3	0.67
June	4		0.54	0.4	0.8	0.65	0.35
July	3		0.91	0.7	1.2	1.04	0.45
August	3		0.64	0.6	0.65	0.62	0.05
September	3		0.55	0.38	0.7	0.6	0.3
June–September			0.7				

Note: *n* is the number of observations; *s* is proportion of microsites in mire microlandscapes; Me is the median; min, max, \bar{x} are the minimum, maximum, and mean values of methane flux; σ is the standard deviation; June–September is the value for the summer-autumn observation period.

The analysis of results obtained in 2016 revealed that the main contribution to the methane flux direction control during the early snowless periods was made by temperature of the upper peat horizon ($r = 0.48$, $p = 0.04$) and thaw depth ($r = 0.8$, $p = 0.005$). In 2016 the first signs of methane emission from the palsa surface to the atmosphere were registered at the thaw depth of 14 cm (Fig. 2). Subsequently, a decrease in the vertical methane flux to the near-zero values was registered at the thaw depth equal to 25 cm. Thus, the thaw depth determined the period of the active methane emission from the peat mound surface, which amounted to 18 days in 2016. The autumn methane accumulation at the depth >10 cm is probably explained by maintaining high biomass of methane-producing archaea. According to the molecular-genetic studies, the number of archaea per gram of dry peat in the flat permafrost peatland of the Bol'shezemel'skaya tundra in the lower parts of the seasonally thawed layer (10–60 cm) is two orders of magnitude higher than in the upper 10 cm [6].

The obtained average values of the methane flux from the palsa mire (Table 2) agree with the results of studying other bogs in the permafrost zone. The most similar values were those for the methane emission

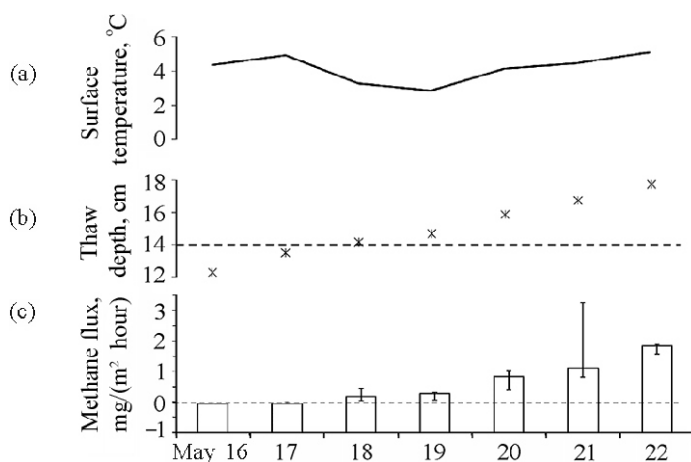


Fig. 2. The dynamics of (a) peat surface temperature, (b) thaw depth, and (c) methane flux from the palsa during the early snowless period in 2016. The bars in the diagram correspond to the median of daily fluxes from the surface of different palsa elements ($n = 6$), the lower value of the error bar is the 1st quartile, and the upper value is the 3rd quartile.

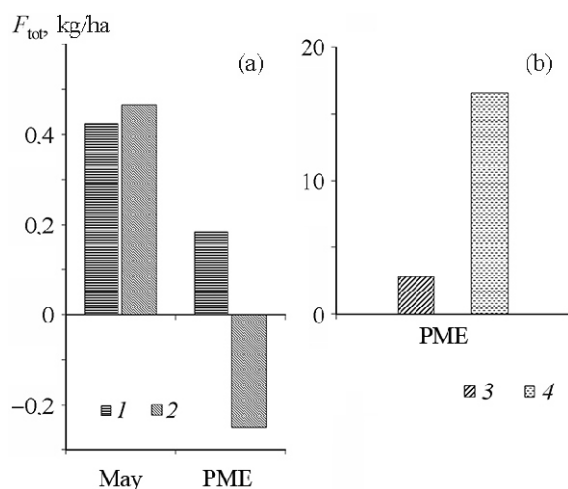


Fig. 3. Total carbon loss due to the methane emission from (a) the communities of the palsa, (b) shrub-sphagnum ridges and cotton-grass-sphagnum hollows in May (18 days) and over the period of active methane emission (PME, 163 days) in 2016. (1) Peat spots; (2) lichen communities; (3) shrub-sphagnum communities; (4) cotton-grass-sphagnum communities.

from the surface of elevated areas of wetlands (palsas and shrub ridges) [16, 24]. Differences in the rate of fluxes are more strongly pronounced for grassy fen microsites of peatlands [15, 16, 22]. High spatial variability of methane emission in the communities in depressions at permafrost wetlands in Canada, Sweden, and Russia is primarily associated with the diversity of plants species and with differences in hydrothermal conditions.

The calculations of total seasonal emission (equation (2)) were used to determine the contribution of typical microsites to the total carbon loss in the form of methane in the analyzed area of the palsa mire in the extreme northern taiga zone. In 2016, during the period of the intense methane flux (18 days) in spring, 0.42 kg CH₄/ha was emitted from the surface of the palsa peat spots, and 0.46 kg CH₄/ha, from the lichen and shrub-lichen communities (Fig. 3). In the next summer-autumn period, the greenless peat spots with the methane emission lost insignificant amount of carbon (0.18 kg CH₄/ha), and the sink was observed in the lichen communities (–0.25 kg CH₄/ha).

About 2.8 kg CH₄/ha was emitted to the atmosphere from shrub-sphagnum ridges over the period of the active methane emission (163 days). Maximum carbon loss was registered in cotton-grass-sphagnum hol-

lows: 16.5 kg CH₄/ha (Fig. 3). Total methane loss in the analyzed part of the mire (11 ha) over the period of active methane emission amounted to 0.7 t or 65 kg CH₄/ha.

Thus, the annual emission of methane from the palsa mire is determined by the intensity of its flux from fens and hollows (80% of the total one). Assuming that the summer-autumn period describes 77% of the annual methane flux from the surface of a similar mire [19], the ecosystem of the analyzed mire can lose about 0.9 t of methane per year, or 81 kg CH₄/(ha year). Permafrost peat mounds with the lichen and shrub-lichen cover in their modern state remain a carbon reservoir and are characterized by insignificant methane emission. However, the disturbance of the ground cover and hydrothermal conditions at the mounds can change this balance of greenhouse gas fluxes.

CONCLUSIONS

The main source of atmospheric methane on the palsa mire in the extreme northern taiga zone in the European part of Russia in May to August in 2016 was hollows. The amount of methane emitted to the atmosphere from the cotton-grass-sphagnum hollows was 16.5 kg CH₄/ha, and the carbon loss due to the methane emission from the shrub-sphagnum ridges was six times smaller.

The rate of the methane flux on the greenless peat spots was equal to 0.03–0.26 mg CH₄/(m² hour), and the seasonal loss was 0.18 kg CH₄/ha. The lichen and shrub-lichen communities during the period of active emission in 60% of cases performed as a sink of 0.25 CH₄/ha. In general, palsas with the preserved ground cover were a reservoir for the methane carbon. The intense methane flux from the palsa was registered at the end of May at the thaw depth of 14 cm. Over the short period (18 days), the spring flux from the palsa surface amounted to 0.42–0.46 kg CH₄/ha, at the absolute emission rate of 0.02–3.8 mg CH₄/(m² hour). However, the revelation of reasons for the active methane emission from the palsa in spring requires long-term observations. The results can be used for verifying regional climate change models.

FUNDING

The present study is performed within the research theme of the Institute of Biology of Komi Scientific Center (Ural Branch, Russian Academy of Sciences (RAS)) AAAA-A17-117122090014-8 “Spatiotemporal Dynamics of Structure and Productivity of Phytocenoses of Forest and Wetland Ecosystems in Northeastern European Russia” and the complex program for basic research of the Ural Branch of RAS (project number 18-4-4-17 “Vertical Fluxes of Carbonaceous Greenhouse Gases in Boreal Forest and Wetland Ecosystems in Modern Climate”).

REFERENCES

1. *The Atlas of Climate and Hydrology for the Komi Republic* (Drofa, Moscow, 1997) [in Russian].
2. S. E. Vomperskii, A. A. Sirin, O. P. Tsyganova, N. A. Valyaeva, and D. A. Maikov, “Bogs and Wetlands in Russia: An Attempt to Analyze the Spatial Distribution and Diversity,” *Izv. Akad. Nauk, Geogr.*, No. 5 (2005) [in Russian].
3. L. I. Vorob'eva, *Archaea, Training Manual for Universities* (Akademkniga, Moscow, 2007) [in Russian].
4. *Geocryological Map of the USSR*, Ed. by E. D. Ershov and K. A. Kondrat'ev (Min-vo Geologii SSSR, MGU, Moscow, 1998) [in Russian].
5. *Komi Center for Hydrometeorology and Environmental Monitoring. Weather in Petrun'*, <http://meteork.ru/climate/petrun.shtml> (Accessed February 19, 2019).
6. E. M. Lapteva, Yu. A. Vinogradova, T. I. Chernov, V. A. Kovaleva, and E. M. Perminova, “Structure and Diversity of Soil Microbial Communities in Palsa Mires in the Northwest of Bol'shezemel'skaya Tundra,” *Izv. Komi NTs URO RAN*, No. 4 (2017) [in Russian].
7. A. V. Pastukhov, T. I. Marchenko-Vagapova, D. A. Kaverin, and N. N. Goncharova, “Genesis and Evolution of Palsa Mires in the Sporadic Permafrost Area in the European Northeast (Middle Basin of the Kosyu River),” *Kriosfera Zemli*, No. 1, **20** (2016) [in Russian].
8. N. I. P'yavchenko, *Peatbogs, Their Natural and Economic Significance* (Nauka, Moscow, 1985) [in Russian].
9. *Vegetation in the European Part of the USSR* (Nauka, Leningrad, 1980) [in Russian].
10. A. F. Sabrekov, M. V. Glagolev, I. E. Kleptsova, V. N. Bashkin, P. A. Barsukov, and Sh. Sh. Maksyutov, “Contribution of Palsa to Methane Emission from West Siberian Tundra Wetlands,” *DOS i GIK*, No. 2, **2** (2011) [in Russian].
11. G. G. Suvorov and M. V. Glagolev, “Duration of the “Methane Emission Period,” in *Wetlands and Biosphere: Proceedings of the Sixth Scientific School (September 10–14, 2007)* (Tomskii TsNTI, Tomsk, 2007) [in Russian].

12. A. P. Shennikov, *Introduction to Geobotany* (LGU, Leningrad, 1964) [in Russian].
13. G. B. Avery, R. D. Shannon, J. R. White, C. S. Martens, and M. J. Alperin, "Effect of Seasonal Change in the Pathway of Methanogenesis on the ^{13}C Values of Pore Water Methane in a Michigan Peatland," *Global Biogeochem. Cycles*, **6** (1999).
14. J. Bosio, M. Johansson, T. V. Callaghan, B. Johansen, and T. R. Christensen, "Future Vegetation Changes in Thawing Subarctic Mires and Implications for Greenhouse Gas Exchange—A Regional Assessment," *Climatic Change*, No. 2, **115** (2012).
15. J. L. Bubier, T. R. Moore, L. Bellisario, N. T. Comer, and P. M. Crill, "Ecological Controls on Methane Emissions from a Northern Peatland Complex in the Zone of Discontinuous Permafrost, Manitoba, Canada," *Global Biogeochem. Cycles*, No. 4, **9** (1995).
16. J. E. Heikkinen, T. Virtanen, J. T. Huttunen, V. V. Elsakov, and P. J. Martikainen, "Carbon Balance in East European Tundra," *Global Biogeochem. Cycles*, No. 1, **18** (2004).
17. M. Helbig, W. L. Quinton, and O. Sonnentag, "Warmer Spring Conditions Increase Annual Methane Emissions from a Boreal Peat Landscape with Sporadic Permafrost," *Environ. Res. Lett.*, No. 11, **12** (2017).
18. G. Hugelius, J. Strauss, S. Zubrzycki, J. W. Harden, E. Schuur, Chien-Lu Ping, L. Schirrmeyer, G. Grosse, G. J. Michaelson, C. D. Koven, J. O'Donnell, B. Elberling, U. Mishra, P. Camill, Zicheng Yu, J. Palmag, and P. Kuhry, "Estimated Stocks of Circumpolar Permafrost Carbon with Quantified Uncertainty Ranges and Identified Data Gaps," *Biogeosciences* (Online), No. 23, **11** (2014).
19. M. Jackowicz-Korczynski, T. R. Christensen, K. Backstrand, P. M. Crill, T. Friborg, M. Mastepanov, and L. Strom, "Annual Cycle of Methane Emission from a Subarctic Peatland," *J. Geophys. Res.*, **115** (2010).
20. X. Liu, Y. Guo, H. Hu, C. Sun, X. Zhao, and C. Wei, "Dynamics and Controls of CO_2 and CH_4 Emissions in the Wetland of a Montane Permafrost Region, Northeast China," *Atmos. Environ.*, **122** (2015).
21. M. Luoto, S. Fronzek, and F. S. Zuidhoff, "Spatial Modelling of Palsa Mires in Relation to Climate in Northern Europe," *Earth Surface Processes and Landforms*, No. 11, **29** (2004).
22. A. Malhotra and N. T. Roulet, "Environmental Correlates of Peatland Carbon Fluxes in a Thawing Landscape: Do Transitional Thaw Stages Matter?," *Biogeosciences*, No. 10, **12** (2015).
23. C. K. McCalley, B. J. Woodcroft, S. B. Hodgkins, R. A. Wehr, E.-H. Kim, R. Mondav, P. M. Crill, J. P. Chanton, V. I. Rich, G. W. Tyson, and S. R. Saleska, "Methane Dynamics Regulated by Microbial Community Response to Permafrost Thaw," *Nature*, No. 7523, **514** (2014).
24. S. C. Moosavi, P. M. Crill, E. R. Pullman, D. Funk, and K. Peterson, "Controls on CH_4 Flux from an Alaskan Boreal Wetland," *Global Biogeochem. Cycles*, No. 2, **10** (1996).
25. H. Nykanen, J. E. Heikkinen, L. Pirinen, K. Tiilikainen, and P. J. Martikainen, "Annual CO_2 Exchange and CH_4 Fluxes on Subarctic Palsa Mire during Climatically Different Years," *Global Biogeochem. Cycles*, No. 1, **17** (2003).
26. J. Rinne, T. Riiutta, M. Pihlatie, M. Aurela, S. Haapanala, J.-P. Tuovinen, E. Tuittila, and T. Vesala, "Annual Cycle of Methane Emission from a Boreal Fen Measured by the Eddy Covariance Technique," *Tellus B*, No. 3, **59** (2007).
27. J. P. Schimel, "Plant Transport and Methane Production as Controls on Methane Flux from Arctic Wet Meadow Tundra," *Biogeochemistry*, **28** (1995).
28. J. Schneider, H. F. Jungkunst, U. Wolf, P. Schreiber, M. Gazovic, M. Miglovets, O. Mikhaylov, D. Grunwald, S. Erasmi, M. Wilmking, and L. Kutzbach, "Russian Boreal Peatlands Dominate the Natural European Methane Budget," No. 1, **11** (2016).
29. E. A. G. Schuur, A. D. McGuire, C. Schaedel, G. Grosse, J. W. Harden, D. Hayes, G. Hugelius, C. Koven, P. Kuhry, D. Lawrence, S. Natali, D. Olefeldt, V. Romanovsky, K. Schaefer, M. Turetsky, C. Treat, and J. Von, "Climate Change and the Permafrost Carbon Feedback," *Nature*, **520** (2015).
30. A. Sirin, T. Minayeva, T. Yurkovskaya, O. Kuznetsov, V. Smagin, and Yu. Fedorov, "Russian Federation (European Part)," in *Mires and Peatlands of Europe: Status, Distribution and Conservation*, Ed. by H. Joosten, F. Tanneberger, and A. Moen (Schweizerbart Science Publishers, Stuttgart, 2017).
31. D. Wagner, C. Wille, S. Kobabe, and E. M. Pfeiffer, "Simulation of Freezing-thawing Cycles in a Permafrost Microcosm for Assessing Microbial Methane Production under Extreme Conditions," *Permafrost and Periglacial Processes*, No. 4, **14** (2003).
32. G. J. Whiting and J. P. Chanton, "Plant-dependent CH_4 Emission in a Subarctic Canadian Fen," *Global Biogeochem. Cycles*, **6** (1992).